ChemPubSoc Europe

DOI: 10.1002/chem.201504719

CHEMISTRY A European Journal Full Paper

Porphyrinoids |*Hot Paper*|

Boron Arylations of Subporphyrins with Aryl Zinc Reagents

Ryota Kotani, Kota Yoshida, Eiji Tsurumaki, and Atsuhiro Osuka*[a]

Abstract: Boron arylations of *B*-(methoxo)triphenylsubporphyrin have been developed with a combined use of ArZnI·LiCl and trimethylsilyl chloride. Aryl zinc reagents bearing bromo, cyano, amide, and ester groups can be employed for the *B*-arylation reaction to provide the corresponding *B*-arylated subporphyrins in moderate yields. Post-modifications of *B*-arylated subporphyrins have been demonstrated without loss of the B–C bond. These modifications include conversion of the cyano group into a benzoyl group with PhMgBr, hydrolysis of the ester group to give *B*-(4-carboxyphenyl)subporphyrin, and Pd-catalyzed Suzuki–Miyaura coupling of the 4-bromophenyl group to give a 1,4-phenylene-bridged subporphyrin–Zn^{II} porphyrin hybrid that displays intramolecular excitation energy transfer from the subporphyrin to the porphyrin. The newly synthesized *B*-arylated subporphyrins have been fully characterized by NMR, UV/Vis absorption and fluorescence spectroscopies, mass spectrometry, electrochemical measurements, and X-ray diffraction analysis.

Introduction

In recent years, subporphyrins, ring-contracted porphyrin cousins coordinating a boron atom in the central cavity with a bowl-shaped distorted 14π aromatic system, have emerged as promising functional pigments in light of their tunable photophysical and electrochemical properties, high fluorescence quantum yields, and large nonlinear optical responses.[1] Rational fabrications of subporphyrins have been accomplished mostly at the *meso*- and β-positions so far. *meso*-Aryl substituents of subporphyrins can rotate rather freely to provide large substituent effects, and the introduction of various *meso*-aryl substituents has led to the creation of subporphyrins possessing versatile electronic properties.[2] Along this strategy, many A_3-type *meso*-aryl-substituted subporphyrins have been prepared. Representative examples include *meso*-(oligophenyleneethynylene)-substituted subporphyrins[3] that display expanded π-conjugated chromophores and *meso*-(4-aminophenyl)-substituted subporphyrins[4] that exhibit remarkable quinonoidal contributions. *meso*-Bromosubporphyrin has been used for the synthesis of lower symmetry A_2B-type subporphyrins, some of which undergo efficient electron-transfer and excitation-energy-transfer reactions.[5] β-Mono- and perhalogenations of subporphyrins have been demonstrated, and the resultant β-halogenated subporphyrins underwent various substitution reactions to provide the corresponding products.[6] As interesting examples, β-hexaphenylethynylated subporphyrin was prepared from β-hexabromosubporphyrin[6b] and exhibited a large two-photon absorption cross-section, and tris(1,4-benzodithiino)subporphyrin were prepared from β-hexachlorosubporphyrin and displayed a large association constant to capture C_{60}.[6c]

In contrast, chemical modifications of the axial group of subporphyrins have been only poorly explored.[7] Recently, we reported subporphyrin *B*-hydrides by the reaction of *B*-(methoxo)triphenylsubporphyrin **1** with diisobutylaluminum hydride as a rare example of porphyrinoid borohydrides.[7c] We also succeeded in the isolation of subporphyrinatoborenium cation $\mathbf{2}^+$ as a salt with a carborane anion, $[CH_6B_{11}Br_6]^-$, which was shown to be a planar structure (Scheme 1).[7a] The borenium cation $\mathbf{2}^+$ was then converted into *B*-phenylated subporphyrin **3** upon treatment with PhLi. Shortly after this work, *B*-arylations of **1** were achieved by reactions with organomagne-

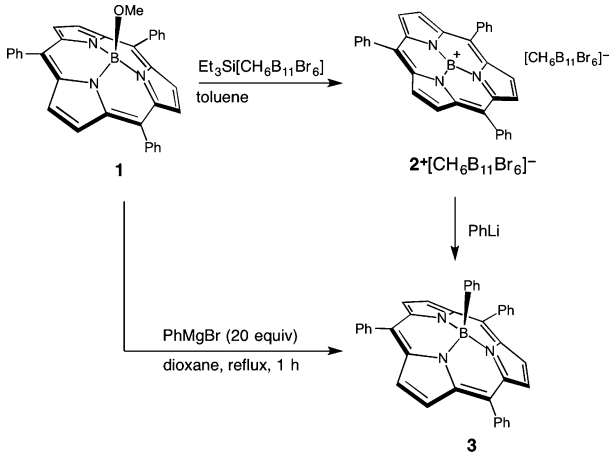

Scheme 1. Synthesis of *B*-phenylated subporphyrin **3**.

[a] *R. Kotani, K. Yoshida, Dr. E. Tsurumaki, Prof. Dr. A. Osuka*
Department of Chemistry, Graduate School of Science
Kyoto University, Sakyo-ku, Kyoto 606-8502 (Japan)
Fax: (+81) 75-753-3970
E-mail: osuka@kuchem.kyoto-u.ac.jp

Supporting information for this article is available on the WWW under http://dx.doi.org/10.1002/chem.201504719.

sium reagents as a more facile synthetic route to *B*-arylated subporphyrins.[8] However, the scope of this *B*-arylation is limited because of the high nucleophilicity of aryl magnesium bromides. It is desirable to expand the scope of the axial aryl groups of subporphyrins, including various functional groups. We thus examined *B*-arylation reactions of subporphyrins with aryl zinc reagents because aryl zinc reagents are milder carbon nucleophiles with much wider functional-group compatibility than aryl magnesium reagents.[9]

Results and Discussion

ArZnI·LiCl reagents (hereafter abbreviated as ArZn reagents) were prepared by direct insertion of Zn powder into iodoarenes in the presence of LiCl.[10] As an initial attempt, *B*-phenylation of **1** with 20 equivalents of PhZn reagent was carried out under the same conditions as those used for *B*-arylation of **1** with Grignard reagents (Table 1, entry 1). However, this attempt resulted in a low yield of *B*-phenylsubporphyrin **3**, and starting material **1** was mostly recovered, probably due to the low nucleophilicity of the PhZn reagent. In order to activate **1** for nucleophilic attack of the PhZn reagent, we examined the addition of 20 equivalents of TMSCl, because the presence of a Lewis acid facilitated boron axial exchange reactions.[11] This indeed improved the yield of **3** dramatically (Scheme 2; Table 1, entry 2), although Lewis acids such as ZnI_2 and $ZnBr_2$ were not effective for the B-phenylation (Table 1, entries 3 and 4). If the reaction was carried out at room temperature, the yield of **3** dropped to 57% (Table 1, entry 5), although a longer reaction time gave a better result (Table 1, entry 6). Moreover, B-phenylation with a lower amount of PhZn reagent (5 equiv) at room temperature gave a cleaner reaction mixture, from which the separation of **3** was easier, with a 77% yield after isolation (Table 1, entry 7). A further decrease in the amount of PhZn reagent (1.5 equiv) lowered the yield of **3** (Table 1, entry 8). Therefore, we concluded that the reaction conditions in entry 7 in Table 1, (5 equiv of PhZn reagent, 20 equiv of TMSCl, THF as solvent, room temperature, 16 h) were the best. In the course of the optimization of the reaction conditions, we noticed that the *B*-trimethylsiloxy-substituted subporphyrin **4** was formed as a side product (Table 1, entries 2 and 5–8). Side product **4** was isolated and its structure was elucidated by X-ray crystallographic analysis (see the Supporting Information). The ^{1}H NMR spectrum of **4** displays a singlet due to the TMS group at $\delta = -1.10$ ppm, which is high-field shifted by the strong diatropic ring current of the subporphyrin. The ^{11}B NMR spectrum of **4** displays a singlet at $\delta = -16.7$ ppm, which is high-field shifted relative to that of **1** ($\delta = -15.3$ ppm)[2c] due to the larger electron-donating effect of the trimethylsiloxy group.

Table 1. *B*-Phenylation of **1** with phenylzinc reagent.

Entry	Lewis acid	n[a]	T [°C]	t [h]	Yield of **3**[b] [%]
1[c]	none	20	reflux	1	5
2	TMSCl	20	60	1	81
3	ZnI_2	20	60	1	N.D. [d]
4	$ZnBr_2$	20	60	1	N.D. [d]
5	TMSCl	20	RT	1	57
6	TMSCl	20	RT	16	74
7	TMSCl	5	RT	16	79 (77[e])
8	TMSCl	1.5	RT	16	66

[a] n: Equivalents of PhZn reagent. [b] Yields were determined by ^{1}H NMR spectroscopy with diphenylmethane as an internal standard. [c] Dioxane was used as a solvent. [d] N.D.: not determined. [e] Yield of isolated product.

1 **3**

Scheme 2. *B*-Phenylation of **1** with phenylzinc reagent. TMSCl: trimethylsilyl chloride.

With the optimized reaction conditions in hand, we then synthesized novel *B*-aryl-substituted subporphyrins (Scheme 3). *B*-(4-Cyanophenyl)-, *B*-(4-(ethoxycarbonyl)phenyl)-, *B*-(4-(piperidine-1-carbonyl)phenyl)-, and *B*-(4-bromophenyl)-substituted subporphyrins **5**–**8** were obtained in moderate yields by the reaction of **1** with the corresponding ArZn reagents. The yields of **5**–**7** were lower than that of **3**, presumably because of the poorer nucleophilicity of ArZn reagents bearing electron-withdrawing groups. Furthermore, we examined postmodifications of the *B*-aryl substituents. Nucleophilic addition of PhMgBr (10 equiv) to **5** at 60 °C followed by hydrolysis with aqueous HCl provided *B*-(4-(benzoyl)phenyl)-substituted subporphyrin **9** in 42% yield. When treated with PhMgBr under reflux conditions, **1** was converted into **3**, whereas **5** was not converted into **3**, which indicated that the axial B–C bond is more robust than the B–O bond under these conditions. Hydrolysis of the ester group in subporphyrin **6** under basic conditions provided *B*-(4-carboxyphenyl)-substituted subporphyrin **10** in 87% yield. Finally, 1,4-phenylene-bridged subporphyrin–porphyrin hybrid **11** was synthesized in 79% yield by the Suzuki–Miyaura cross-coupling reaction of **8** with 5-(4′,4′,5′,5′-tetramethyl-1′,3′,2′-dioxaboran-2-yl)-10,20-diphenylporphyrinato zinc(II)[12] with the aid of a SPhos Pd G2 precatalyst.[13]

Single crystals suitable for X-ray diffraction analysis were obtained by slow recrystallizations from CH_2Cl_2/methanol solutions of **5**, **6**, and **8**, from benzene/*n*-heptane solutions of **7** and **10**, from a CH_2Cl_2/*n*-hexane solution of **9**, and from a $CHCl_3$/*n*-hexane solution of **11**. The crystal structures are shown in Figure 1 (see also the Supporting information). The axial B–C bond lengths of **5**–**11** were in the range of 1.61–1.63 Å, which are similar to those in *B*-aryl subporphyrins previously reported.[8] The bowl depths, which are defined as the distance from the mean plane of the peripheral six β carbon atoms to the center boron atom, are in the range of 1.31–1.43 Å. It is likely that the bowl depths are variable and depend upon the packing structures. Carboxylic acid **10** re-

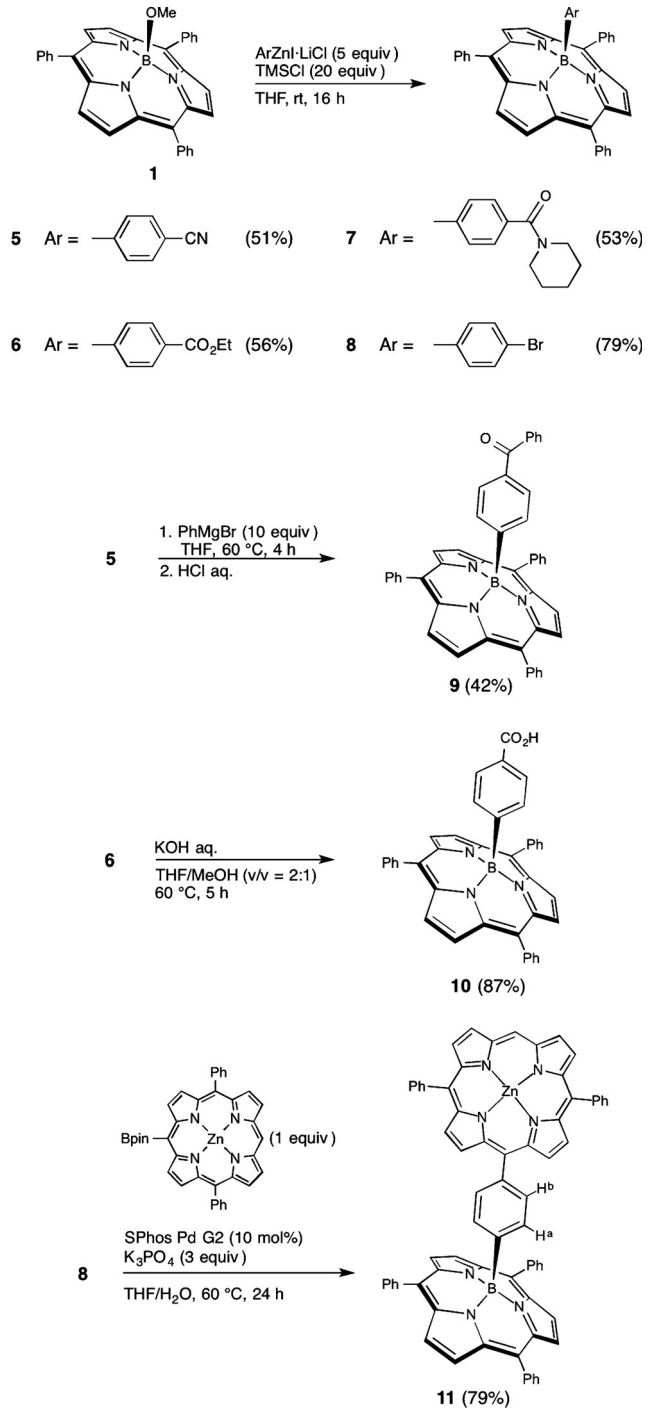

Scheme 3. Synthesis of *B*-arylated subporphyrins and their subsequent conversions. SPhos Pd G2: 2-dicyclohexylphosphino-2′,6′-dimethoxybiphenyl Pd second-generation catalyst.

vealed a face-to-face dimeric packing structure, in which two subporphyrin molecules are connected by hydrogen-bonding interactions with the carboxylic groups (Figure 1 g). Both intermolecular O···O distances are 2.615 Å. The C=O and C–O bond lengths on the CO_2H part of **10** are 1.228(4) and 1.306(4) Å, values that are slightly longer and shorter than the corresponding C=O and C–O bond lengths in ester **6** (1.208(2) and 1.3437(19) Å), respectively, and indicate effective hydrogen bonding. In hybrid **11**, the Zn^{II} porphyrin and subporphyrin parts are linked through a 1,4-phenylene bridge with a center-to-center (zinc-to-boron) distance of 9.32 Å.

The ^{1}H NMR spectrum of *B*-(4-bromophenyl)subporphyrin **8** shows a singlet at $\delta = 8.16$ ppm due to the six β protons, a set of three signals at $\delta = 8.06$, 7.70, and 7.61 ppm due to the *meso*-phenyl protons, and two doublets at $\delta = 6.44$ and 4.50 ppm due to the axial *B*-phenylene protons. Similarly, the ^{1}H NMR spectra of the other *B*-aryl subporphyrins (**5**–**7** and **9**–**11**) show the aromatic protons in the *B*-aryl groups at high-field chemical shifts (2,6-protons at $\delta = 4.3$–5.0 ppm and 3,5-protons at $\delta = 6.5$–7.2 ppm), which indicate diatropic ring currents due to the 14π-electronic aromatic circuits (see also the Supporting Information). The ^{1}H NMR spectrum of subporphyrin–porphyrin hybrid **11** exhibits signals due to the H^a and H^b protons at $\delta = 5.01$ and 7.17 ppm, respectively, which reflect the diatropic ring currents of the subporphyrin and porphyrin.

The electrochemical potentials of **5**–**11** were measured by cyclic voltammetry and differential-pulse voltammetry in CH_2Cl_2 containing 0.10 M nBu_4NPF_6 as a supporting electrolyte (see Table 2 and the Supporting Information). Subporphyrin

Table 2. Oxidation and reduction potentials of subporphyrins **1**, **3**, and **5**–**11** (vs. the ferrocene/ferricenium ion pair). Supporting electrolyte: nBu_4NPF_6 (0.10 M); working electrode: glassy carbon; counter electrode: platinum wire; reference electrode: $Ag/AgClO_4$; scan rate: 0.05 V s^{-1}.

	$E_{ox.2}$ [V]	$E_{ox.1}$ [V]	$E_{red.1}$ [V]	$E_{red.2}$ [V]	$E_{ox.1}-E_{red.1}$ [a] [eV]
1[b]		0.82	−1.84		2.66
3[b]		0.58	−2.01		2.59
5		0.72	−2.07[c]		2.79
6		0.67	−2.13[c]		2.80
7		0.65	−2.12[c]		2.77
8		0.66	−1.96		2.62
9		0.65	−2.08[c]		2.73
10		0.66	−2.11[c]		2.77
11	0.65[c]	0.30[c]	−1.92[c]	−2.03[c]	2.22

[a] Electrochemical HOMO–LUMO gap. [b] Ref. [2c]. [c] Determined by differential-pulse voltammetry.

1 shows reversible reduction and oxidation potentials at −1.84 and 0.82 V.[8] However, *B*-phenylsubporphyrin **3** exhibits reversible reduction and oxidation potentials at lower potentials of −2.01 and 0.58 V, respectively, which reflect the electron-donating phenyl substituent rather than the methoxy group.[7a] Subporphyrins **5**–**10** exhibit similar reversible oxidation potentials to **3**, although their reduction waves are irreversible except for that of **8**. The electrochemical HOMO–LUMO gaps for **5**–**10** are larger than that for **3**, in contrast to those of subporphyrins bearing electron-donating *B*-aryl groups.[8] These results are consistent with density functional theory calculations performed at the B3LYP/6-311G(d) level by using the Gaussian 09 package (see the Supporting Information).[14] Subporphyrin–porphyrin hybrid **11** shows a first one-electron oxidation at 0.30 V and a second two-electron oxidation at 0.65 V. The two-electron oxidation process has been interpreted in

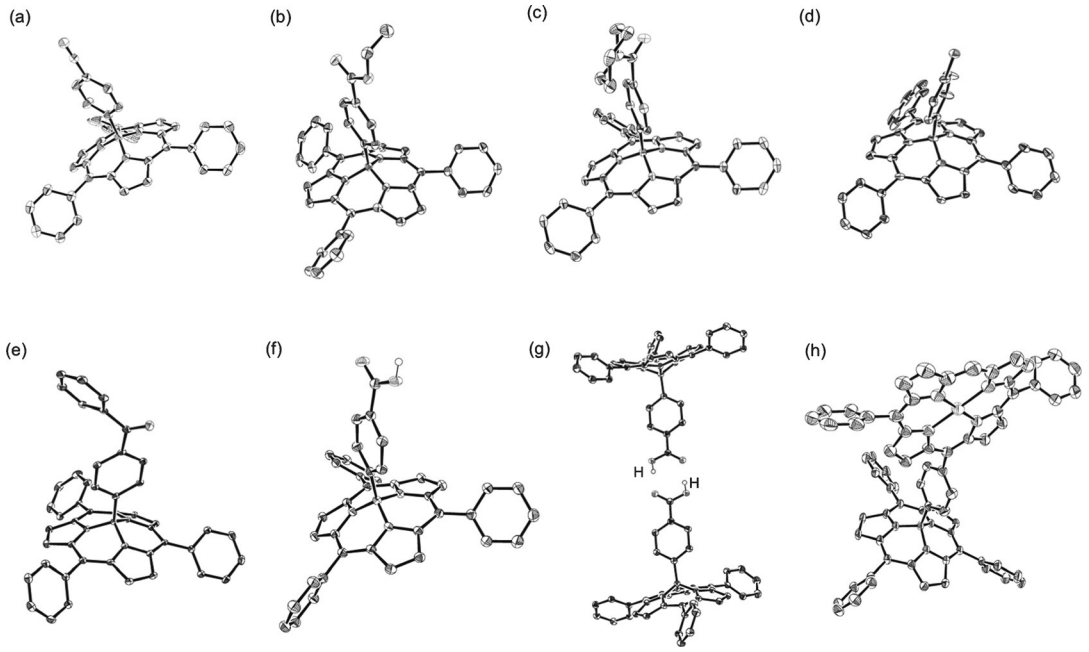

Figure 1. X-Ray crystal structures of (a) **5**, (b) **6**, (c) **7**, (d) **8**, (e) **9**, (f) **10**, and (h) **11**. (g) Dimeric packing structure of **10**. Thermal ellipsoids are set to 50% probability level. Hydrogen atoms except for the OH proton in **10** and solvent molecules are omitted for clarity.

terms of overlap of the first oxidation of the subporphyrin unit and the second oxidation of the Zn porphyrin unit. The first and the second reductions of **11** were observed at −1.92 and −2.03 V, respectively, as reversible waves, which indicates the electronic deconjugation nature of the subporphyrin and porphyrin units.

The UV/Vis absorption and fluorescence spectra of **5**–**10** are quite similar to those of **3** and reveal Soret-like bands in the range of 383–384 nm, Q-like bands at around 506 nm, and fluorescence maxima at around 540 nm with quantum yields of $\Phi_F = 0.12$–0.13 (Table 3).[8] 4-Bromophenyl-substituted subporphyrin **8** shows a similar fluorescence quantum yield, despite the presence of the bromine substituent. As shown in Figure 2a, the absorption spectrum of **11** is almost the superposition of those of **3** and 5,10,15-tris(3,5-di-*tert*-butylphenyl)-porphyrinatozinc(II) (**12**), which indicates negligible electronic interaction in the ground state. The fluorescence spectrum of **11** taken for excitation of the subporphyrin at 386 nm shows

Table 3. Optical properties of subporphyrins **1**, **3**, and **5**–**11** measured in CH_2Cl_2.

	λ [nm] (ε [10^5 M^{-1} cm^{-1}])			λ_{em}[a] [nm]	Φ_F[a]
1[b]	372 (1.66)	460 (0.12)	485 (0.09)	517	0.13
3[c]	385 (1.55)	481 (0.10)	507 (0.15)	545	0.16
5	383 (1.57)	479 (0.09)	507 (0.13)	541	0.12
6	384 (1.47)	478 (0.09)	506 (0.14)	540	0.13
7	384 (1.46)	478 (0.09)	506 (0.14)	543	0.13
8	384 (1.40)	479 (0.09)	506 (0.13)	542	0.12
9	384 (1.41)	478 (0.09)	506 (0.13)	543	0.13
10	384 (1.43)	478 (0.09)	506 (0.13)	541	0.12
11	386 (1.78) 506 (0.15)	414 (5.00) 542 (0.20)	476 (0.10)	545, 584, 634 (584, 634)[d]	0.02[c] (0.03)[d]

[a] Fluorescence spectra were recorded upon excitation at the peak maxima of Soret-like bands of subporphyrins (372–386 nm). [b] Ref. [2c]. [c] Ref. [7a]. [d] Values in brackets were obtained upon excition at 414 nm.

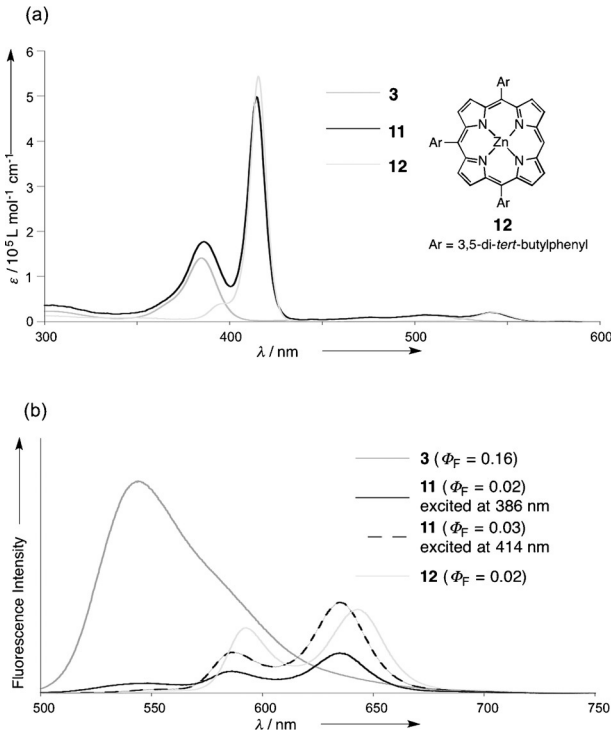

Figure 2. (a) UV/Vis absorption spectra and (b) fluorescence spectra of subporphyrins **3**, subporphyrin–porphyrin dyad **11**, and porphyrin **12** in CH_2Cl_2.

decreased fluorescence (545 nm) due to the subporphyrin and increased fluorescence (584 and 634 nm) due to the Zn^{II}–porphyrin; this reveals intramolecular excitation energy transfer from the subporphyrin moiety to the porphyrin moiety. From a comparison of the fluorescence spectra of **3** and **11**, the quantum efficiency for the energy transfer of **11** is estimated to be $\Phi_{ET}=0.97$, which is slightly smaller than that ($\Phi_{ET}\approx1.00$) of a previously reported *meso*-phenylene-bridged subporphyrin–porphyrin dyad.[15] If **11** was excited at 414 nm, which corresponds to the Soret band of the porphyrin moiety, only the fluorescence from the porphyrin unit was observed with $\Phi_F=0.03$.

Conclusion

We have developed a new synthetic protocol for *B*-aryl subporphyrins by using aryl zinc reagents in the presence of trimethylsilyl chloride. Zinc reagents attached to electron-withdrawing groups are available for the reaction, to provide the corresponding *B*-aryl subporphyrins **5**–**8** in moderate yields. Postmodifications of the *B*-aryl substituents were demonstrated to give novel subporphyrins **9**–**11** without loss of the B–C bond. Newly synthesized subporphyrins **5**–**11** were all fully characterized by ^{1}H and ^{11}B NMR spectra and mass spectra, and X-ray diffraction analysis. The electrochemical and photophysical properties of **5**–**10** are comparable to those of **3**. Subporphyrin–porphyrin hybrid **11** exhibits efficient intramolecular energy transfer at excited states. As demonstrated, this synthetic protocol allowed for the synthesis of a wider range of subporphyrins bearing various axial boron subsituents and, hence, opens a way to novel functional subporphyrins. Further applications of this method to more elaborated subporphyrin-based molecular systems are actively being pursued in our laboratory.

Experimental Section

General information

All reagents and solvents were of commercial reagent grade and were used without further purification unless noted. THF and dioxane were purified with a solvent purification system before use. ^{1}H, ^{11}B, and ^{13}C NMR spectra were recorded on a JEOL ECA-600 spectrometer. Chemical shifts were expressed as the δ scale in ppm relative to the internal standard $CHCl_3$ ($\delta=7.26$ ppm for ^{1}H, and $\delta=77.16$ ppm for ^{13}C) and an external standard $BF_3{\cdot}OEt_2$ in $CDCl_3$ ($\delta=0.00$ ppm for ^{11}B). Spectroscopic grade solvents were used for all spectroscopic studies without further purification. UV/Vis absorption spectra were recorded on a Shimadzu UV-2500 spectrometer. Fluorescence spectra were recorded on a Shimadzu RF-5300PC spectrometer. Absolute fluorescence quantum yields were determined on a HAMAMATSU C9920–02S instrument. High-resolution atmospheric-pressure-chemical-ionization time-of-flight mass spectroscopy (HR-APCI-TOF-MS) was performed on a BRUKER micrOTOF model by using positive mode. X-Ray data were taken at $-180\,^\circ$C with a Rigaku XtaLAB P200 apparatus and two-dimensional PILATUS 100 K/R detector with CuK_α radiation ($\lambda=1.54187$ Å). The structures were solved by the SIR-97 direct method and refined with the SHELXL-97 program.[16] Thin-layer chromatography was performed with silica gel 60 F_{254}. Preparative separations were performed with silica gel chromatography (Wako gel C-300). Redox potentials were measured on an ALS electrochemical analyzer model 660.

General procedure for the synthesis of ArZn reagents

ArZn reagents used in the reactions were prepared according to reference [10].

General procedure for the synthesis of *B*-arylated subporphyrins

A solution of **1** ($\approx$60 μmol) in THF (1 mL) was cooled to 0 °C with an ice bath. After dropwise addition of TMSCl (0.15 mL, 1.2 mmol) through a syringe, a THF solution ofArZnI·LiCl (0.30 mmol) was added to the mixture, and the solution was stirred for 16 h at room temperature. The reaction mixture was poured onto water and extracted with AcOEt. The organic layer was washed with brine and dried over Na_2SO_4, and the solvent was removed under reduced pressure. The crude product was separated by silica gel column chromatography. Recrystallization furnished the corresponding *B*-arylated subporphyrin.

Phenyl(5,10,15-triphenyllsubporphyrinato)boron(III) (3): According to the general procedure, **3** was prepared from **1** (29.9 mg, 59.6 μmol) and ArZnI·LiCl (Ar: phenyl; 0.98 M, 0.31 mL, 0.30 mmol). The crude product was separated by silica gel column chromatography (eluent: *n*-hexane/CH_2Cl_2, 3:1). Recrystallization from CH_2Cl_2/MeOH furnished **3** (25.0 mg, 77%) as an orange solid. The chemical properties of **3** were in accordance with those previously reported.[8a]

Trimethylsiloxo(5,10,15-triphenylsubporphyrinato)boron(III) (4): This compound was obtained as a side product under the above *B*-arylation conditions. Selective preparation of **4** was as follows: *B*-(Hydroxo)triphenylsubporphyrin (20.1 mg, 41.2 μmol) in THF (1 mL) was added to TMSCl (0.10 mL, 0.80 mmol), and the mixture was stirred for 30 min at room temperature. The crude product was purified by silica gel column chromatography (eluent: *n*-hexane/CH_2Cl_2, 4:1). Recrystallization from CH_2Cl_2/*n*-hexane furnished **4** (8.4 mg, 36%) as an orange solid. A single crystal suitable for X-ray diffraction analysis was prepared by slow recrystallization from CH_3Cl/*n*-heptane. ^{1}H NMR (600 MHz, $CDCl_3$): $\delta=8.09$–8.07 (12H, β and *meso*-Ph *ortho*), 7.71 (t, $J=7.8$ Hz, 6H, *meso*-Ph *meta*), 7.61 (t, $J=7.7$ Hz, 3H, *meso*-Ph *para*), and -1.10 ppm (s, 9H, trimethyl); ^{11}B NMR (193 MHz, $CDCl_3$): $\delta=-16.7$ ppm (s, 1B).

4-Cyanophenyl(5,10,15-triphenylsubporphyrinato)boron(III) (5): According to the general procedure, **5** was prepared from **1** (31.5 mg, 62.8 μmol) and ArZnI·LiCl (Ar: 4-cyanophenyl; 0.78 M, 0.40 mL, 0.31 mmol). The crude product was separated by silica gel column chromatography (eluent: *n*-hexane/CH_2Cl_2/diethyl ether, 8:4:1). Recrystallization from CH_2Cl_2/MeOH furnished **5** (18.3 mg, 51%) as an orange solid. A single crystal suitable for X-ray diffraction analysis was prepared by slow recrystallization from CH_2Cl_2/MeOH. ^{1}H NMR (600 MHz, $CDCl_3$): $\delta=8.18$ (s, 6H, β), 8.06 (d, $J=8.2$ Hz, 6H, *meso*-Ph *ortho*), 7.71 (t, $J=7.8$ Hz, 6H, *meso*-Ph *meta*), 7.63 (t, $J=7.8$ Hz, 3H, *meso*-Ph *para*), 6.59 (d, $J=8.2$ Hz, 2H, axial-Ar *meta*), 4.69 ppm (d, $J=8.7$ Hz, 2H, axial-Ar *ortho*); ^{11}B NMR (193 MHz, $CDCl_3$): $\delta=-16.7$ ppm (s, 1B); ^{13}C NMR (150 MHz, $CDCl_3$): $\delta=140.5$, 137.2, 133.3, 129.9, 129.2, 128.9, 128.0, 122.6, 120.8, 119.4, 109.2 ppm (no signal was observed for the carbon atom directly bonded to the boron atom); HR-APCI TOF-MS: *m/z* calcd for $C_{40}H_{25}{}^{11}BN_4$ $[M+H]^+$: 573.2252; found: 573.2269; UV/Vis (in CH_2Cl_2): λ (ε) = 383 (157000), 479 (9000), 507 nm

(14000 $M^{-1}cm^{-1}$); fluorescence (in CH_2Cl_2, $\lambda_{ex}=383$ nm); $\lambda_{max}=541$ nm, $\Phi_F=0.12$.

4-(Ethoxycarbonyl)phenyl(5,10,15-triphenylsubporphyrinato)boron(III) (6): According to the general procedure, **6** was prepared from **1** (29.8 mg, 59.4 μmol) and ArZnI·LiCl (Ar: 4-(ethoxycarbonyl)-phenyl; 0.64 M, 0.49 mL, 0.30 mmol). The crude product was separated by silica gel column chromatography (eluent: *n*-hexane/CH_2Cl_2/diethyl ether, 8:4:1). Recrystallization from CH_2Cl_2/MeOH furnished **6** (20.8 mg, 56%) as an orange solid. A single crystal suitable for X-ray diffraction analysis was prepared by slow recrystallization from CH_2Cl_2/MeOH. ^{1}H NMR (600 MHz, $CDCl_3$): $\delta=8.17$ (s, 6H, β), 8.07 (d, $J=7.3$ Hz, 6H, *meso*-Ph *ortho*), 7.70 (t, $J=7.8$ Hz, 6H, *meso*-Ph *meta*), 7.62 (t, $J=7.3$ Hz, 3H, *meso*-Ph *para*), 7.00 (d, $J=8.2$ Hz, 2H, axial-Ar *meta*), 4.71 (d, $J=8.3$ Hz, 2H, axial-Ar *ortho*), 4.06 (q, $J=7.2$ Hz, 2H, CH_2), 1.12 ppm (t, $J=6.9$ Hz, 3H, CH_3); ^{11}B NMR (193 MHz, $CDCl_3$): $\delta=-16.5$ ppm (s, 1B); ^{13}C NMR (150 MHz, $CDCl_3$): $\delta=166.8$, 140.5, 137.4, 133.4, 128.8, 128.7, 127.9, 127.4, 122.5, 120.7, 120.6, 60.3, 14.3 ppm (no signal was observed for the carbon atom directly bonded to the boron atom); HR-APCI-TOF-MS: *m/z* calcd for $C_{42}H_{30}{}^{11}BN_3O_2$ $[M+H]^+$: 620.2511; found: 620.2502; UV/Vis (in CH_2Cl_2): λ (ε)=384 (147000), 478 (9000), 506 nm (14000 $M^{-1}cm^{-1}$); fluorescence (in CH_2Cl_2, $\lambda_{ex}=384$ nm): $\lambda_{max}=540$ nm, $\Phi_F=0.13$.

4-(Piperidine-1-carbonyl)phenyl(5,10,15-triphenylsubporphyrinato)boron(III) (7): According to the general procedure, **7** was prepared from **1** (30.2 mg, 60.2 μmol) and ArZnI·LiCl (Ar: 4-(pyperidine-1-carbonyl)phenyl; 0.76 M, 0.39 mL, 0.30 mmol). The crude product was separated by silica gel column chromatography (eluent: *n*-hexane/CH_2Cl_2/EtOAc, 8:1:1). Recrystallization from CH_2Cl_2/MeOH furnished **7** (21.0 mg, 53%) as an orange solid. A single crystal suitable for X-ray diffraction analysis was prepared by slow recrystallization from benzene/*n*-heptane. ^{1}H NMR (600 MHz, $CDCl_3$): $\delta=8.16$ (s, 6H, β), 8.08 (d, $J=7.6$ Hz, 6H, *meso*-Ph *ortho*), 7.72 (t, $J=7.7$ Hz, 6H, *meso*-Ph *meta*), 7.61 (t, $J=7.3$ Hz, 3H, *meso*-Ph *para*), 6.32 (d, $J=8.3$ Hz, 2H, axial-Ar *meta*), 4.64 (d, $J=7.7$ Hz, 2H, axial-Ar *ortho*), 3.43 (m, 2H, piperidyl), 2.87 (m, 2H, piperidyl), 1.54–1.46 (m, 4H, piperidyl), 1.20 ppm (m, 2H, piperidyl); ^{11}B NMR (193 MHz, $CDCl_3$): $\delta=-16.4$ ppm (s, 1B); ^{13}C NMR (150 MHz, $CDCl_3$): $\delta=170.6$, 140.5, 137.5, 133.8, 133.4, 128.8, 128.7, 127.9, 124.6, 122.4, 120.6, 48.5, 42.8, 26.4, 25.8, 24.6 ppm (no signal was observed for the carbon atom directly bonded to the boron atom); HR-APCI-TOF-MS: *m/z* calcd for $C_{45}H_{35}{}^{11}BN_4O$ $[M+H]^+$: 659.2984; found 659.2988; UV/Vis (in CH_2Cl_2): λ (ε)=384 (146000), 478 (9000), 506 nm (14000 $M^{-1}cm^{-1}$); fluorescence (in CH_2Cl_2, $\lambda_{ex}=384$ nm): $\lambda_{max}=543$ nm, $\Phi_F=0.13$.

4-Bromophenyl(5,10,15-triphenylsubporphyrinato)boron(III) (8): According to the general procedure, **8** was prepared from **1** (29.9 mg, 59.6 μmol) and ArZnI·LiCl (Ar: 4-bromophenyl; 0.70 M, 0.43 mL, 0.30 mmol). The crude product was separated by silica gel column chromatography (eluent: *n*-hexane/CH_2Cl_2/diethyl ether, 8:4:1). Recrystallization from CH_2Cl_2/MeOH furnished **8** (29.5 mg, 79%) as an orange solid. A single crystal suitable for X-ray diffraction analysis was prepared by slow recrystallization from CH_2Cl_2/MeOH. ^{1}H NMR (600 MHz, $CDCl_3$): $\delta=8.16$ (s, 6H, β), 8.06 (d, $J=6.8$ Hz, 6H, *meso*-Ph *ortho*), 7.70 (t, $J=7.3$ Hz, 6H, *meso*-Ph *meta*), 7.61 (t, $J=7.4$ Hz, 3H, *meso*-Ph *para*), 6.44 (d, $J=8.3$ Hz, 2H, axial-Ar *meta*), 4.50 ppm (d, $J=8.7$ Hz, 2H, axial-Ar *ortho*); ^{11}B NMR (193 MHz, $CDCl_3$): $\delta=-16.4$ ppm (s, 1B); ^{13}C NMR (150 MHz, $CDCl_3$): $\delta=140.5$, 137.4, 133.4, 130.6, 129.3, 128.8, 127.9, 122.4, 120.6, 120.1 ppm (no signal was observed for the carbon atom directly bonded to the boron atom); HR-APCI-TOF-MS: *m/z* calcd for $C_{39}H_{25}{}^{11}BN_3{}^{79}Br$ $[M+H]^+$: 626.1404; found: 626.1386; UV/Vis (in CH_2Cl_2): λ (ε)=384 (140000), 479 (9000), 506 nm (13000 $M^{-1}cm^{-1}$); fluorescence (in CH_2Cl_2, $\lambda_{ex}=384$ nm); $\lambda_{max}=542$ nm, $\Phi_F=0.12$.

Synthesis of 4-(benzoyl)phenyl(5,10,15-triphenylsubporphyrinato)boron(III) (9)

PhMgBr in THF solution (0.50 mL, 0.50 mmol) was added to a solution of **5** (28.6 mg, 50.0 μmol) in THF (1 mL), and the solution was stirred for 4 h at 60 °C. 1 M aqueous HCl (1 mL) was added, and the mixture was stirred for 20 min at room temperature. The reaction mixture was poured onto water and extracted with AcOEt. The organic layer was washed with brine and dried over Na_2SO_4, and the solvent was removed under reduced pressure. The crude product was separated by silica gel column chromatography (eluent: *n*-hexane/CH_2Cl_2/diethyl ether, 10:3:1). Recrystallization from CH_2Cl_2/MeOH furnished **9** (13.3 mg, 42%) as an orange solid. A single crystal suitable for X-ray diffraction analysis was prepared by slow recrystallization from CH_2Cl_2/*n*-hexane. ^{1}H NMR (600 MHz, $CDCl_3$): $\delta=8.18$ (s, 6H, β), 8.06 (d, $J=6.8$ Hz, 6H, *meso*-Ph *ortho*), 7.71 (t, $J=7.8$ Hz, 6H, *meso*-Ph *meta*), 7.62 (t, $J=7.3$ Hz, 3H, *meso*-Ph *para*) 7.39 (m, 3H, axial-COPh), 7.25 (t, $J=7.8$ Hz, 2H, axial-COPh), 6.77 (d, $J=8.3$ Hz, 2H, axial-Ar *meta*), 4.64 ppm (d, $J=8.3$ Hz, 2H, axial-Ar *ortho*); ^{11}B NMR (193 MHz, $CDCl_3$): $\delta=-16.6$ ppm (s, 1B); ^{13}C NMR (150 MHz, $CDCl_3$): $\delta=196.6$, 140.5, 137.8, 137.3, 135.0, 133.3, 131.8, 129.7, 128.8, 128.6, 128.5, 128.1, 127.9, 122.5, 120.7 ppm (no signal was observed for the carbon atom directly bonded to the boron atom); HR-APCI-TOF-MS: *m/z* calcd for $C_{46}H_{30}{}^{11}BN_3O$ $[M+H]^+$: 652.2562; found: 652.2521; UV/Vis (in CH_2Cl_2): λ (ε)=384 (141000), 478 (9000), 506 nm (13000 $M^{-1}cm^{-1}$); fluorescence (in CH_2Cl_2, $\lambda_{ex}=384$ nm): $\lambda_{max}=543$ nm, $\Phi_F=0.13$.

Synthesis of 4-carboxyphenyl(5,10,15-triphenylsubporpyrinato)boron(III) (10)

1 M aqueous KOH (1 mL) was added to a solution of **6** (25.3 mg, 40.8 μmol) in THF (1 mL) and MeOH (0.5 mL), and the mixture was stirred for 6 h at 60 °C. The solution was quenched by addition of 1 M aqueous HCl (2 mL). The reaction mixture was poured onto water and extracted with AcOEt. The organic layer was washed with brine and dried over Na_2SO_4, and the solvent was removed under reduced pressure. The crude product was separated by silica gel column chromatography (eluent: *n*-hexane/CH_2Cl_2/AcOEt, 2:1:1). Recrystallization from CH_2Cl_2/*n*-hexane furnished **10** (21.1 mg, 87%) as an orange solid. A single crystal suitable for X-ray diffraction analysis was prepared by slow recrystallization from benzene/*n*-heptane. ^{1}H NMR (600 MHz, $CDCl_3$): $\delta=12.5$–10.5 (br, 1H, CO_2H), 8.18 (s, 6H, β), 8.06 (d, $J=6.9$ Hz, 6H, *meso*-Ph *ortho*), 7.69 (t, $J=7.3$ Hz, 6H, *meso*-Ph *meta*), 7.60 (t, $J=7.4$ Hz, 3H, *meso*-Ph *para*), 6.98 (d, $J=8.3$ Hz, 2H, axial-Ar *meta*), 4.69 ppm (d, $J=8.2$ Hz, 2H, axial-Ar *ortho*); ^{11}B NMR (193 MHz, $CDCl_3$): $\delta=-16.7$ ppm (s, 1B); ^{13}C NMR (150 MHz, $CDCl_3$): $\delta=171.3$, 140.5, 137.3, 133.3, 128.8, 128.7, 128.0, 127.9, 126.5, 122.5, 120.7 ppm (no signal was observed for the carbon atom directly bonded to the boron atom); HR-APCI-TOF-MS: *m/z* calcd for $C_{40}H_{26}{}^{11}BN_3O_2$ $[M+H]^+$: 592.2198; found: 592.2206; UV/Vis (in CH_2Cl_2): λ (ε)=384 (143000), 478 (9000), 506 nm (13000 $M^{-1}cm^{-1}$); fluorescence (in CH_2Cl_2, $\lambda_{ex}=384$ nm); $\lambda_{max}=541$ nm, $\Phi_F=0.12$.

Synthesis of subporphyrin–porphyrin dyad 11

A solution of **8** (44.1 mg, 70.4 μmol), 5-pinacolatoboryl-10,20-diphenylporphyrin (42.1 mg, 71.5 μmol), SPhos Pd G2 catalyst (5.0 mg, 6.9 μmol), and K_3PO_4 (45.0 mg, 212 μmol) in THF (1.3 mL) and H_2O (30 μL) was stirred for 24 h at 60 °C. The reaction mixture

was poured onto water and extracted with AcOEt. The organic layer was washed with brine and dried over Na_2SO_4, and the solvent was removed under reduced pressure. The crude product was separated by silica gel column chromatography (eluent: *n*-hexane/CH_2Cl_2/diethyl ether, 4:1:1). Recrystallization from CH_2Cl_2/MeOH furnished **11** (59.8 mg, 79%) as a purple solid. A single crystal suitable for X-ray diffraction analysis was prepared by slow recrystallization from $CHCl_3$/*n*-hexane. ^{1}H NMR (600 MHz, $CDCl_3$): $\delta = 10.16$ (s, 1H, porphyrin-*meso*), 9.32 (d, $J = 4.6$ Hz, 2H, porphyrin-β), 9.00 (d, $J = 4.6$ Hz, 2H, porphyrin-β), 8.74 (d, $J = 4.6$ Hz, 2H, porphyrin-β), 8.46 (d, $J = 4.6$ Hz, 2H, porphyrin-β), 8.29 (s, 6H, subporphyrin-β), 8.22 (d, $J = 7.3$ Hz, 6H, subporphyrin-*meso*-Ph *ortho*), 8.13 (d, $J = 6.9$ Hz, 4H, porphyrin-*meso*-Ph *ortho*), 7.76 (t, $J = 7.8$ Hz, 6H, subporphyrin-*meso*-Ph *meta*), 7.73–7.69 (m, 6H, porphyrin-*meso*-Ph *meta* and *para*), 7.65 (t, $J = 7.3$ Hz, 3H, subporphyrin-*meso*-Ph *para*), 7.17 (d, $J = 7.8$ Hz, 2H, axial-Ar *meta*), 5.01 ppm (d, $J = 7.8$ Hz, 2H, axial-phenylene *ortho*); ^{11}B NMR (193 MHz, $CDCl_3$): $\delta = -16.2$ ppm (s, 1B); ^{13}C NMR (150 MHz, $CDCl_3$): $\delta = 150.0$, 149.9, 149.8, 142.8, 140.8, 139.9, 137.7, 134.6, 133.5, 132.9, 132.5, 132.4, 132.1, 131.6, 131.5, 131.3, 128.8, 127.9, 127.5, 126.9, 126.6, 122.5, 122.4, 120.8, 120.4 ppm (no signal was observed for the carbon atom directly bonded to the boron atom); HR-APCI-TOF-MS: *m/z* calcd for $C_{71}H_{44}{}^{11}BN_7{}^{64}Zn$ $[M+H]^+$: 1070.3127; found: 1070.3075; UV/Vis (in CH_2Cl_2): λ (ε): 386 (178000), 414 (500000), 476 (10000), 506 (15000), 542 nm (20000 $M^{-1}cm^{-1}$); fluorescence (in CH_2Cl_2, $\lambda_{ex} =$ 386 nm): $\lambda_{max} = 545$, 584, 634 nm, $\Phi_F = 0.03$; (in CH_2Cl_2, $\lambda_{ex} =$ 414 nm): $\lambda_{max} = 584$, 634 nm, $\Phi_F = 0.02$.

Acknowledgements

This work was supported by JSPS KAKENHI (Grant numbers 25220802 and 25620031).

Keywords: boron–carbon bonds · energy transfer · organozinc reagents · porphyrinoids · subporphyrins

[1] a) Y. Inokuma, A. Osuka, *Dalton Trans.* **2008**, 2517; b) T. Torres, *Angew. Chem. Int. Ed.* **2006**, *45*, 2834; *Angew. Chem.* **2006**, *118*, 2900; c) A. Osuka, E. Tsurumaki, T. Tanaka, *Bull. Chem. Soc. Jpn.* **2011**, *84*, 679; d) C. G. Claessens, D. Gonzáles-Rodríguez, M. S. Rodríguez-Morgade, A. Medina, T. Torres, *Chem. Rev.* **2014**, *114*, 2192.

[2] a) N. Kobayashi, Y. Takeuchi, A. Matsuda, *Angew. Chem. Int. Ed.* **2007**, *46*, 758; *Angew. Chem.* **2007**, *119*, 772; b) Y. Takeuchi, A. Matsuda, N. Kobayashi, *J. Am. Chem. Soc.* **2007**, *129*, 8271; c) Y. Inokuma, Z. S. Yoon, D. Kim, A. Osuka, *J. Am. Chem. Soc.* **2007**, *129*, 4747.

[3] Y. Inokuma, S. Easwaramoorthi, S. Y. Jang, K. S. Kim, D. Kim, A. Osuka, *Angew. Chem. Int. Ed.* **2008**, *47*, 4840; *Angew. Chem.* **2008**, *120*, 4918.

[4] Y. Inokuma, S. Easwaramoorthi, Z. S. Yoon, D. Kim, A. Osuka, *J. Am. Chem. Soc.* **2008**, *130*, 12234.

[5] a) M. Kitano, S.-y. Hayashi, T. Tanaka, H. Yorimitsu, N. Aratani, A. Osuka, *Angew. Chem. Int. Ed.* **2012**, *51*, 5593; *Angew. Chem.* **2012**, *124*, 5691; b) M. Kitano, S.-y. Hayashi, T. Tanaka, N. Aratani, A. Osuka, *Chem. Eur. J.* **2012**, *18*, 8929; c) D. Shimizu, H. Mori, M. Kitano, W.-Y. Cha, J. Oh, T. Tanaka, D. Kim, A. Osuka, *Chem. Eur. J.* **2014**, *20*, 16194.

[6] a) S. Zhao, C. Liu, Y. Guo, J. C. Xiao, Q. Y. Chen, *Synthesis* **2014**, *46*, 2499; b) E. Tsurumaki, Y. Inokuma, S. Easwaramoorthi, J. M. Lim, D. Kim, A. Osuka, *Chem. Eur. J.* **2009**, *15*, 237; c) K. Yoshida, A. Osuka, *Chem. Asian J.* **2015**, *10*, 1526.

[7] a) E. Tsurumaki, S.-y. Hayashi, F. S. Tham, C. A. Reed, A. Osuka, *J. Am. Chem. Soc.* **2011**, *133*, 11956; b) S. Shimizu, A. Matsuda, N. Kobayashi, *Inorg. Chem.* **2009**, *48*, 7885; c) E. Tsurumaki, J. Sung, D. Kim, A. Osuka, *J. Am. Chem. Soc.* **2015**, *137*, 1056.

[8] S. Saga, S.-y. Hayashi, K. Yoshida, E. Tsurumaki, P. Kim, Y. M. Sung, J. Sung, T. Tanaka, D. Kim, A. Osuka, *Chem. Eur. J.* **2013**, *19*, 11158.

[9] a) "Polyfunctional Zinc Organometallics for Organic Synthesis": P. Knochel, H. Leuser, L.-Z. Gong, S. Perrone, F. F. Kneisel, *Handbook of Functionalized Organometallics Vol. 1* (Ed.: P. Knochel), Wiley-VCH, Weinheim, **2005**, p. 251; b) *Organozinc Reagents* (Eds.: P. Knochel, P. Jones), Oxford University Press, New York, **1999**.

[10] A. Krasovskiy, V. Malakhov, A. Gavryushin, P. Knochel, *Angew. Chem. Int. Ed.* **2006**, *45*, 6040; *Angew. Chem.* **2006**, *118*, 6186.

[11] a) J. Guilleme, D. Gonzáles-Rodríguez, T. Torres, *Angew. Chem. Int. Ed.* **2011**, *50*, 3506; *Angew. Chem.* **2011**, *123*, 3568; b) M. Kitano, Y. Okuda, E. Tsurumaki, T. Tanaka, H. Yorimitsu, A. Osuka, *Angew. Chem. Int. Ed.* **2015**, *54*, 9275; *Angew. Chem.* **2015**, *127*, 9407.

[12] A. G. Hyslop, M. A. Kellett, P. M. Iovine, M. J. Therien, *J. Am. Chem. Soc.* **1998**, *120*, 12676.

[13] W. Shu, S. L. Buchwald, *Chem. Sci.* **2011**, *2*, 2321.

[14] Gaussian 09, Revision A.02, M. J. Frisch, G. W. Trucks, H. B. Schlegel, G. E. Scuseria, M. A. Robb, J. R. Cheeseman, G. Scalmani, V. Barone, B. Mennucci, G. A. Petersson, H. Nakatsuji, M. Caricato, X. Li, H. P. Hratchian, A. F. Izmaylov, J. Bloino, G. Zheng, J. L. Sonnenberg, M. Hada, M. Ehara, K. Toyota, R. Fukuda, J. Hasegawa, M. Ishida, T. Nakajima, Y. Honda, O. Kitao, H. Nakai, T. Vreven, J. A. Montgomery, Jr., J. E. Peralta, F. Ogliaro, M. Bearpark, J. J. Heyd, E. Brothers, K. N. Kudin, V. N. Staroverov, R. Kobayashi, J. Normand, K. Raghavachari, A. Rendell, J. C. Burant, S. S. Iyengar, J. Tomasi, M. Cossi, N. Rega, J. M. Millam, M. Klene, J. E. Knox, J. B. Cross, V. Bakken, C. Adamo, J. Jaramillo, R. Gomperts, R. E. Stratmann, O. Yazyev, A. J. Austin, R. Cammi, C. Pomelli, J. W. Ochterski, R. L. Martin, K. Morokuma, V. G. Zakrzewski, G. A. Voth, P. Salvador, J. J. Dannenberg, S. Dapprich, A. D. Daniels, Ö. Farkas, J. B. Foresman, J. V. Ortiz, J. Cioslowski, D. J. Fox, Gaussian, Inc. Wallingford CT, **2009**.

[15] a) Y. Inokuma, S.-y. Hayashi, A. Osuka, *Chem. Lett.* **2009**, *38*, 206; b) J. Oh, J. Sung, M. Kitano, Y. Inokuma, A. Osuka, D. Kim, *Chem. Commun.* **2014**, *50*, 10424. For related subporphyrin-based hybrid systems showing intramolecular-energy-transfer phenomena, see: c) H. Sugimoto, M. Muto, T. Tanaka, A. Osuka, *Eur. J. Org. Chem.* **2011**, 71; d) T. Xu, R. Lu, X. Liu, P. Chen, X. Qiu, Y. Zhao, *Eur. J. Org. Chem.* **2008**, 1065.

[16] SHELXL-97 and SHELXS-97, Program for the Refinement of Crystal Structures from Diffraction Data, University of Göttingen, Göttingen (Germany); G. M. Sheldrick, T. R. Schneider, *Methods Enzymol.* **1997**, *277*, 319.

Received: November 24, 2015
Published online on January 27, 2016

